between first and second Al-H BDEs in the parent compound, AlH_3.

The presence of the unsymmetrical monobridged structure of Al_2H_2 as a genuine minimum proves that this structural type is not limited to Si_2H_2,[8,14] for which solid experimental structural confirmation now exists.[12] This work surely suggests that related potential energy hypersurfaces—B_2H_2, $BAlH_2$, $BGaH_2$, $AlGaH_2$, Ga_2H_2, $SiCH_2$, Ge_2H_2, $GeCH_2$, $GeSiH_2$—should be carefully searched for new unsymmetrical monobridged structures.

Acknowledgment. We thank Seung-Joon Kim, Yukio Yamaguchi, and Yaoming Xie for many helpful discussions. This research was supported by the U.S. Air Force Office of Scientific Research, Grant AFOSR-92-J-0047.

$PO_3^-\cdot(H_2O)_n$ Clusters. Molecular Anion Structures, Energetics, and Vibrational Frequencies

Buyong Ma, Yaoming Xie, Mingzuo Shen, and Henry F. Schaefer, III*

Contribution from the Center for Computational Quantum Chemistry, The University of Georgia, Athens, Georgia 30602. *Received July 20, 1992*

Abstract: The $PO_3^-\cdot(H_2O)_n$ clusters (n = 1, 2, and 3) have been studied using ab initio quantum mechanical methods. Self-consistent field (SCF), configuration interaction with single and double excitations (CISD), and coupled cluster single and double excitation (CCSD) levels of theory were employed in conjunction with basis sets of quality double-zeta (DZ), double-zeta plus polarization (DZP), and DZP plus diffuse functions. The most important finding is that the clusters prefer to form high-symmetry double donor–double acceptor hydrogen bonds between the PO_3^- anion and the H_2O molecules. The hydrogen bond lengths increase and the dissociation energies decrease with the addition of successive water molecules. The hydrogen bond in $PO_3^-\cdot H_2O$ has a dissociation energy (D_0 = 13.3 kcal mol^{-1}) about 0.5 kcal mol^{-1} less than that for $NO_3^-\cdot H_2O$. The D_{3h} $PO_3^-\cdot(H_2O)_3$ theoretical results do not agree with the experimental thermochemistry concerning the nature of the hydration of $PO_3^-\cdot(H_2O)_2$ by the third water molecule. The latter finding is consistent with the conclusions of Keesee and Castleman.

1. Introduction

Beginning with the experiments of Henchman, Viggiano, Paulson, Freedman, and Wormhoadt,[1] the metaphosphate anion, PO_3^-, has been shown to be relatively stable and unreactive in the gas phase.[2] However, there is strong laboratory evidence that the PO_3^- anion does not exist as a free entity in aqueous solution,[3] unlike its nitrogen congener NO_3^-. This fact, together with the well-known role of PO_3^- in biological systems[4] and interesting features associated with its bonding and electronic structure,[5] has given impetus to several theoretical and experimental studies. Very recently, experiments have established that PO_3^- is a weaker base than I^- and that PO_3^- is one of the least reactive bases to have been characterized thermodynamically.[6] Therefore, it is important to understand the unusual behavior of PO_3^- in the gaseous phase. The key reactions with water are[2]

$$PO_3^- + (H_2O)_n \rightarrow PO_3^-\cdot(H_2O)_n$$

$$PO_3^-\cdot(H_2O)_n + H_2O \rightarrow H_2PO_4^-\cdot(H_2O)_n$$

The intermediate clusters $PO_3^-\cdot(H_2O)_n$ are very important to the understanding of the properties of PO_3^- in both the gaseous and solution phases. Experimentally it has been shown[1] that the $PO_3^-\cdot(H_2O)_n$ clusters are stable in the gaseous phase and that the isomerization barrier varies with the number of water molecules, n. Unfortunately, there is no theoretical research concerning the $PO_3^-\cdot(H_2O)_n$ clusters. Although there is considerable laboratory thermochemical data from the important work of Keesee and Castleman,[2] there is very little experimental structural information concerning PO_3^- and its clusters. In fact, since $PO_3^-\cdot(H_2O)_{n+1}$ and $H_2PO_4^-\cdot(H_2O)_n$ are indistinguishable by mass spectrometry, there may be some uncertainty about the nature of the observed clustering as well as the isomerization behavior of PO_3^-.

Since the hydrogen bonding in the $NO_3^-\cdot H_2O$ system has been investigated previously,[7,8] the current study attempts to make meaningful comparisons between the hydration behaviors of PO_3^- and NO_3^-. This paper will consider the structures and properties of the $PO_3^-\cdot(H_2O)_n$ clusters, for n = 0, 1, 2, and 3. Such a theoretical investigation was explicitly called for in the 1989 laboratory study of Keesee and Castleman.[2]

2. Theoretical Methods

The basis sets adopted here include STO-3G (minimum basis set),[9] double-zeta (DZ),[10,11] double-zeta plus polarization (DZP),[12] and DZP plus diffuse functions (DZP+diff) for the P and O atoms. The basis set denoted DZP for hydrogen is the (4s/2s) set[8] with the set of p functions having orbital exponents $\alpha_p(H)$ = 0.75; for the oxygen and phosphorus atoms we chose the Huzinaga–Dunning–Hay bases[10-12] O(9s5p/4s2p),

(1) Henchman, M.; Viggiano, A. A.; Paulson, J. F.; Freedman, A.; Wormhoadt, J. *J. Am. Chem. Soc.* **1985**, *107*, 1453.
(2) Keesee, R. G.; Castleman, A. W., Jr. *J. Am. Chem. Soc.* **1989**, *111*, 9015.
(3) (a) Jencks, W. P. *Acc. Chem. Res.* **1980**, *13*, 161. (b) Ramirez, F.; Marecek, J.; Minore, J.; Srivastava, S.; leNoble, W. *J. Am. Chem. Soc.* **1986**, *108*, 348. (c) Burgess, J.; Blundell, N.; Cullis, P. M.; Hubbard, C. D.; Misra, R. *J. Am. Chem. Soc.* **1988**, *110*, 7900. (d) Freeman, S.; Friedman, J. M.; Knowles, D. *J. Am. Chem. Soc.* **1987**, *109*, 3166. (e) Cullis, P. M.; Nicholls, D. *J. Chem. Soc., Chem. Commun.* **1987**, 783.
(4) Westheimer, F. H. *Chem. Rev.* **1981**, *81*, 313. Westheimer, F. H. *Science* **1987**, *235*, 1173. Related systems of biological significance have been the subject of many theoretical studies, for example: Pullman, A.; Berthod, H.; Gresh, N. *Chem. Phys. Lett.* **1975**, *33*, 11.
(5) Rajca, A.; Rice, J. E.; Streitwieser, A., Jr.; Schaefer, H. F. *J. Am. Chem. Soc.* **1987**, *109*, 4189.
(6) Viggiano, A. A.; Henchman, M. J.; Dale, F.; Deakyne, C. A.; Paulson, J. F. *J. Am. Chem. Soc.* **1992**, *114*, 4299.
(7) Shen, M.; Xie, Y.; Schaefer, H. F.; Deakyne, C. A. *J. Chem. Phys.* **1990**, *93*, 3379.
(8) Shen, M.; Xie, Y.; Schaefer, H. F.; Deakyne, C. A. *Chem. Phys.* **1991**, *151*, 187.
(9) Hehre, W. J.; Stewart, R. F.; Pople, J. A. *J. Chem. Phys.* **1969**, *51*, 2659.
(10) Huzinaga, S. *J. Chem. Phys.* **1965**, *42*, 1293.
(11) Dunning, T. H. *J. Chem. Phys.* **1970**, *53*, 2823.

0002-7863/93/1515-1943$04.00/0

Table I. Theoretical Total Energies, Equilibrium Geometries, and Vibrational Frequencies for PO_3^- (Figure 1)

	DZ SCF	DZP SCF	DZP+diff SCF	DZP CISD	DZP+diff CISD	DZP CCSD	DZP+diff CCSD
total energy, au	−565.224 36	−565.483 64	−565.494 19	−566.037 56	−566.058 22	−566.124 74	−566.149 93
R_e(P–O), Å	1.561	1.464	1.465	1.482	1.484	1.495	1.498
harmonic vib freq, cm^{-1}							
A_1' (P–O stre)		1136	1129				
E′ (P–O stre)		1426	1407				
E′ (bend)		544	537				
A_2'' (umbrella)		556	549				

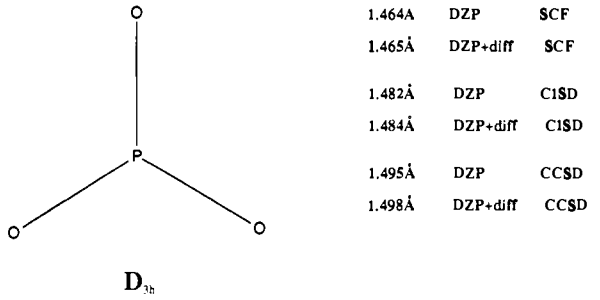

Figure 1. Theoretical equilibrium geometries for the metaphosphate anion, PO_3^-.

P(11s7p/6s4p) with five pure spherical d functions used as polarization functions, the orbital exponents being $\alpha_d(O) = 0.85$, and $\alpha_d(P) = 0.6$. The diffuse functions include both s and p functions on the heavy atoms and have orbital exponents[13,14] $\alpha_s(O) = 0.0845$, $\alpha_p(O) = 0.0845$, $\alpha_s(P) = 0.0348$, and $\alpha_p(P) = 0.0348$.

The Hartree–Fock or self-consistent field (SCF) approach has been used to locate stationary points for several conformations via analytic first derivative techniques. Subsequently, analytic energy second derivative techniques are used to determine whether each stationary point is a local minimum. Finally, the configuration interaction method with single and double excitations (CISD)[15,16] and the coupled cluster method including single and double excitations (CCSD)[17,18] are used to independently optimize the geometries. For the CISD and CCSD methods, only the valence electrons were explicitly correlated. Thus the core-like (phosphorus 1s, 2s, and 2p; oxygen 1s) SCF molecular orbitals were constrained to be doubly occupied in all configurations. Also the corresponding virtual orbitals were excluded from the CISD and CCSD procedures. With the DZP basis set, the numbers of basis functions for PO_3^-, $PO_3^-\cdot H_2O$, $PO_3^-\cdot(H_2O)_2$, and $PO_3^-\cdot(H_2O)_3$ are 68, 93, 118, and 143, respectively. The CISD wave functions for PO_3^-, $PO_3^-\cdot H_2O$, $PO_3^-\cdot(H_2O)_2$, and $PO_3^-\cdot(H_2O)_3$ included 30 100, 116 632, 318 287, and 709 829 configurations, respectively. With the DZP+diff basis set, the CISD wave functions for PO_3^- and $PO_3^-\cdot H_2O$ include 59 242 and 210 034 configurations, respectively. The computations were carried out using the program PSI developed in this research group.

Basis set superposition errors (BSSE) were not applied in this research. With the DZP SCF method, the BSSE corrections to the $PO_3^-\cdot(H_2O)_n$ dissociation energies are substantial, yielding a significant reduction in the predicted D_e and D_0 values. However, it is known[19] that DZP SCF dissociation energies agree well with experiment for the water dimer and other hydrogen-bonded systems. The reason for this is a consistent approximate cancellation between the effects of basis set incompleteness and electron correlation. Thus the application of BSSE corrections to DZP SCF energetic results is a priori expected to give poor agreement with experiment. Since correlation effects are not too important for the dissociation energies predicted here, the same remarks apply to the CISD and CCSD energetics. Ultimately, of course (for example, the DZP full CI method), the use of the DZP basis set will fail, yielding hydrogen-bonding dissociation energies that are too large when a sufficiently complete description of electron correlation effects is achieved.

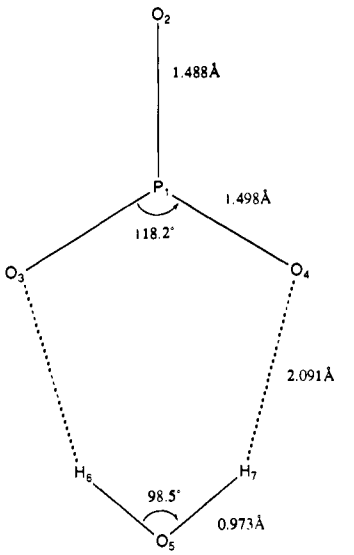

Figure 2. The C_{2v} global minimum equilibrium geometry for $PO_3^-\cdot H_2O$ at the DZP CCSD level of theory.

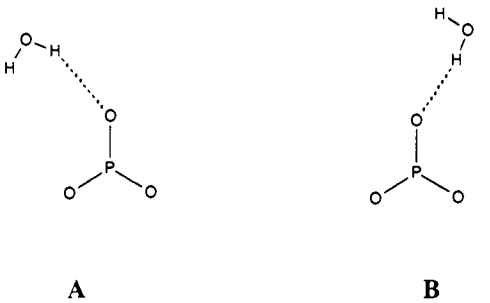

Figure 3. Two closely related conformations of the $PO_3^-\cdot H_2O$ system. Both are minima with the STO-3G SCF method but collapse to the global minimum (Figure 2) when more complete basis sets are used at the SCF level.

3. Results and Discussion

A. Metaphosphate Anion PO_3^-. Our results for the isolated PO_3^- anion are presented in Table I and Figure 1. The introduction of diffuse basis functions lengthens the P–O bond slightly, but electron correlation effects increase the bond length more significantly, i.e., by 0.02 Å with the CISD method, and by 0.03 Å with the CCSD method. As expected, the harmonic vibrational frequencies with the SCF method generally become smaller when the larger DZP+diff basis set is used.

There have been several previous theoretical studies of the metaphosphate anion. For comparison, our most reliable P–O bond length is probably the DZP+diff CISD result, 1.484 Å, which is somewhat longer than previous values of 1.468 Å[20] or

(12) Dunning, T. H.; Hay, P. J. In *Theoretical Chemistry*; Schaefer, H. F., Ed.; Plenum Press: New York, 1977; Vol. 3, p 1.
(13) Clark, T.; Chandrasekhar, J.; Spitznagel, G. W.; Schleyer, P. v. R. *J. Comput. Chem.* **1983**, *4*, 294.
(14) Spitznagel, G. W.; Clark, T.; Schleyer, P. v. R. *J. Comput. Chem.* **1987**, *8*, 1109.
(15) Brooks, B. R.; Laidig, W. D.; Saxe, P.; Goddard, J. D.; Yamaguchi, Y.; Schaefer, H. F. *J. Chem. Phys.* **1980**, *72*, 4652.
(16) Rice, J. E.; Amos, R. D.; Handy, N. C.; Lee, T. J.; Schaefer, H. F. *J. Chem. Phys.* **1986**, *85*, 963.
(17) Purvis, G. D.; Bartlett, R. J. *J. Chem. Phys.* **1982**, *76*, 1910.
(18) Scuseria, G. E.; Janssen, C. L.; Schaefer, H. F. *J. Chem. Phys.* **1989**, *89*, 7382.
(19) See, for example: Feller, D. *J. Chem. Phys.* **1992**, *96*, 6104 and references therein.
(20) Lohr, L. L.; Boehm, R. C. *J. Phys. Chem.* **1987**, *91*, 3203.

Table II. Equilibrium Geometries for the Global Minimum Structure of $PO_3^-\cdot H_2O$ (Figure 2)[a]

theoretical level	$r_e(P_1-O_2)$	$r_e(P_1-O_3)$	$r_e(O_3-H_6)$	$r_e(O_5-H_6)$	$\theta_e(O_3-P_1-O_4)$	$\theta_e(H_6-O_5-H_7)$
DZ SCF	1.555	1.562	2.188	0.957	117.2	107.8
DZ CISD	1.580	1.588	2.154	0.974	117.2	106.3
DZ CCSD	1.601	1.610	2.157	0.958	117.3	105.3
DZP SCF	1.458	1.466	2.197	0.952	118.4	101.1
DZP CISD	1.473	1.482	2.107	0.963	118.2	99.5
DZP CCSD	1.488	1.498	2.091	0.973	118.2	98.5
DZP+diff SCF	1.460	1.467	2.216	0.952	118.4	101.5
DZP+diff CISD	1.476	1.484	2.121	0.963	118.2	99.9

[a] All bond distances are in Å and angles in deg.

Table III. Harmonic Vibrational Frequencies (cm^{-1}) for the Global Minimum Structure of $PO_3^-\cdot H_2O$ (Figure 2)

no.	symmetry	mode	DZP SCF	DZP+diff SCF
1	B_1	O–H stretch	4141 (3031)[a]	4138 (3030)[a]
2	A_1	O–H stretch	4084 (2948)	4080 (2945)
3	A_1	H–O–H bend	1846 (1347)	1824 (1332)
4	A_1	P–O stretch	1443 (1446)	1426 (1428)
5	B_1	P–O stretch	1405 (1405)	1392 (1392)
6	A_1	P–O stretch	1136 (1136)	1130 (1130)
7	B_2	puckering	716 (503)	694 (491)
8	A_1	sym def	553 (553)	548 (548)
9	B_2	O–P out-of-plane	545 (568)	539 (557)
10	B_1	O–P–O bend	543 (543)	537 (537)
11	A_2	asym torsion	408 (291)	404 (289)
12	A_1	O···H stretch	378 (271)	365 (262)
13	A_1	O···H stretch	165 (158)	158 (151)
14	B_1	O···H stretch	82 (80)	77 (75)
15	B_2	asym torsion	47 (47)	43 (43)

[a] The values in parentheses refer to $PO_3^-\cdot D_2O$.

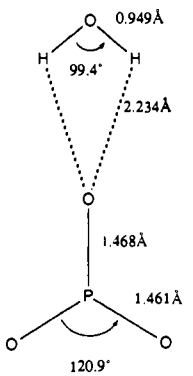

Figure 4. A transition state for $PO_3^-\cdot H_2O$ obtained at the DZP SCF level of theory.

1.475 Å.[5,21] Although the DZP+diff CCSD wave functions are more complete than the DZP+diff CISD, the CCSD method generally requires a larger basis set than DZP+diff for truly quantitative structural predictions. The DZP+diff CCSD total energy is −566.149 93 hartrees (versus −566.087 56 hartrees, the lowest energy reported in earlier theoretical work[20]). Because the main goals of the present study involve the complexes of the metaphosphate anion with water molecule(s), the above results for isolated PO_3^- are presented for comparison and completeness.

B. Metaphosphate Anion–Water Complexes $PO_3^-\cdot H_2O$. We have investigated six arrangements of the metaphosphate anion complex with one water molecule. Two of the arrangements (those sketched in Figure 3) exist only at the minimum basis set (STO-3G) SCF level of theory and collapsed when larger basis sets were used. There are four stationary points on the SCF DZP potential energy surface (Figures 2, 4, 5, and 6). The global minimum is illustrated in Figure 2, and it is the *only* $PO_3^-\cdot H_2O$ minimum located in this research. The structure illustrated in Figure 4 is a transition state, and those illustrated in Figures 5 and 6 both have two imaginary vibrational frequencies.

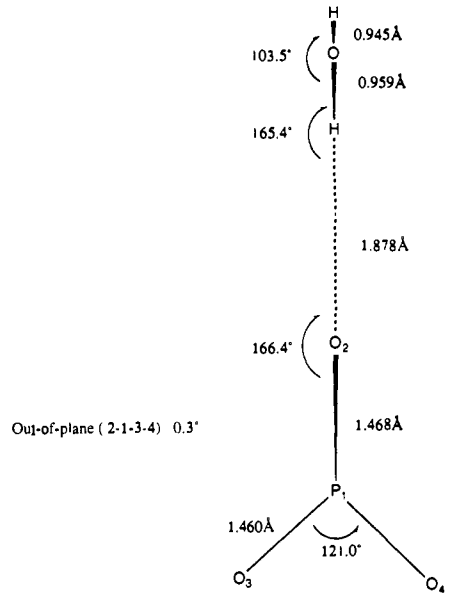

Figure 5. A C_s stationary point (with two imaginary vibrational frequencies) of $PO_3^-\cdot H_2O$ with a single hydrogen bond at the DZP SCF level of theory. The symmetry plane contains the water molecule and the out-of-plane P–O bond.

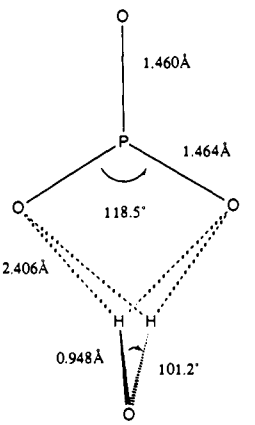

Figure 6. A C_{2v} stationary point (with two imaginary vibrational frequencies) for $PO_3^-\cdot H_2O$ optimized at the DZP SCF level of theory.

The optimized theoretical geometries for the global minimum are presented in Table II, and the harmonic vibrational frequencies and their assignments in Table III. The global minimum of $PO_3^-\cdot H_2O$ incorporates two distinct hydrogen bonds. In Figure 2 we note that, compared with the free anion in Figure 1, the formation of the two hydrogen bonds decreases both the $O_3P_1O_4$ angle in PO_3^- and the $H_6O_5H_7$ angle in H_2O. The bond angle in the isolated water molecule is 106° at the DZP SCF level of theory, while the $H_6O_5H_7$ angle in the complex is 101° at same theoretical level. The $O_3P_1O_4$ bond angle in $PO_3^-\cdot H_2O$ is 2° smaller than the ideal 120° found for the isolated PO_3^- anion. The P_1-O_3 and P_1-O_4 bonds increase by 0.002–0.003 Å with both

(21) O'Keeffe, M.; Domenges, B.; Gibbs, G. V. *J. Phys. Chem.* **1985**, *89*, 2304.

the SCF and CCSD methods, and a change of less than 0.001 Å was found with the CISD method.

Meanwhile, the P_1–O_2 bond, which does not participate in the hydrogen bonding, is about 0.006–0.009 Å shorter than the P–O bond in the free metaphosphate anion at the same theoretical level. Therefore, the PO_3^- moiety in the global minimum of $PO_3^-\cdot H_2O$ exhibits some contribution from the Lewis-type structure[5] i. Note

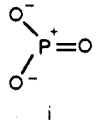

i

that when two hydrogen bonds are required to be connected to only one of the oxygen atoms in PO_3^-, as in Figure 4 (a transition state), then this P–O bond lengthens slightly while the other two became a bit shorter. By the same line of reasoning, the PO_3^- moiety thus incorporated has a greater contribution from the Lewis structure[5] ii. This kind of behavior corroborates the classic Lewis

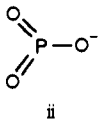

ii

structure of PO_3^- as a resonance hybrid of the two Lewis structures i and ii.

Harmonic vibrational frequencies for the $PO_3^-\cdot H_2O$ complex are reported in Table III. There are some common features concerning the change of vibrational frequencies in $PO_3^-\cdot H_2O$ and $NO_3^-\cdot H_2O$ relative to the isolated PO_3^- and NO_3^- anions. For example, the degeneracy of the E′ (A–O stretch, A = P or N) mode vibrational frequencies of the anions is removed. But in $PO_3^-\cdot H_2O$ the previously degenerate lower E′ (bend) mode frequencies now differ by about 10 cm^{-1}, whereas in the $NO_3^-\cdot H_2O$ system this mode remains essentially degenerate.[7] Also the hydrogen bond in $PO_3^-\cdot H_2O$ is comparable to that in $NO_3^-\cdot H_2O$; this is demonstrated by the three highest "new" vibrational modes: 716 cm^{-1}, 408 cm^{-1}, and 378 cm^{-1} in $PO_3^-\cdot H_2O$ versus 729 cm^{-1}, 316 cm^{-1}, and 210 cm^{-1} in $NO_3^-\cdot H_2O$. However, since frequencies are mass-weighted, a force constant comparison would be more meaningful. The corresponding normal coordinate force constants (mdyn/Å) associated with the "new" modes are 0.345 (716 cm^{-1}), 0.016 (408 cm^{-1}), and 0.013 (378 cm^{-1}) in $PO_3^-\cdot H_2O$, and 0.438 (729 cm^{-1}), 0.014 (316 cm^{-1}), and 0.011 (210 cm^{-1}) in $NO_3^-\cdot H_2O$.

Consistent with the vibrational analysis, there are some differences between the two anions with respect to their potential surfaces.[7,8] Two of the starting arrangements we have used, shown in Figure 3, are analogous to the structures found to be minima at the STO-3G SCF level for $NO_3^-\cdot H_2O$. Both structures A and B (in Figure 3) of $PO_3^-\cdot H_2O$ are also minima at the STO-3G SCF level. However, for $NO_3^-\cdot H_2O$, only structure B remains a minimum at higher levels of theory. In contrast, for $PO_3^-\cdot H_2O$, neither A nor B remains a minimum at higher levels of theory.

For coplanar configurations, the second $PO_3^-\cdot H_2O$ stationary point is a transition state illustrated in Figure 4, which is about 3.2 kcal mol^{-1} higher in energy than the global minimum of Figure 2. There is one imaginary vibrational frequency, corresponding to the movement of the water molecule toward the global minimum. In this structure (Figure 4), the bond angle of H_2O is significantly smaller (99.4°) than that for the isolated water molecule. Since this structure is a transition state, we did not pursue it further with correlated wave functions.

We found only one stationary point that incorporates one conventional monodonor–monoacceptor hydrogen bond, namely, that shown in Figure 5. This structure lies 2.3 kcal mol^{-1} above the global minimum and has two imaginary vibrational frequencies with the DZP SCF method. It is interesting to note that the water H–O–H angle in this structure is still smaller (103.5°) than that of free H_2O (106.3°) at this level of theory, indicating that there is some weak interaction between the second hydrogen atom in water and the oxygen atom in PO_3^-.

From its position in the global minimum (Figure 2), if the H_2O molecule is rotated 90° about the C_2 axis such that the two molecular planes are perpendicular to each other, we find another stationary point with two imaginary vibrational frequencies; this structure is shown in Figure 6. This configuration is about 5.6 kcal mol^{-1} higher in energy than the $PO_3^-\cdot H_2O$ global minimum (Figure 2).

It should be mentioned that, for all the structures discussed above, their total energies are lower than the sum of the separated PO_3^- and H_2O, even though they have energies above that of the global minimum and have one or more imaginary vibrational frequencies on their SCF potential energy surfaces.

The total energies and dissociation energies for the $PO_3^-\cdot(H_2O)_n$ clusters are reported in Table VII, in which the energy differences upon the formation of the clusters are defined as follows:

$PO_3^-\cdot(H_2O)_n$:

$$n = 1 \qquad D_e = E(PO_3^-) + E(H_2O) - E(PO_3^-\cdot H_2O)$$

$$n = 2 \qquad D_e = E(PO_3^-) + 2E(H_2O) - E(PO_3^-\cdot(H_2O)_2)$$

$$n = 3 \qquad D_e = E(PO_3^-) + 3E(H_2O) - E(PO_3^-\cdot(H_2O)_3)$$

For the SCF and CCSD methods, E is the total energy as indicated above. However, for the CISD method, the total energies of the asymptotic system $PO_3^-\cdots(H_2O)_n$ are used instead of the sum of the separated energies, owing to the lack of size consistency in the CISD method. For the asymptote, the intermolecular distances between the PO_3^- anion and the H_2O molecules are 500 bohrs, and the geometries of the PO_3^- anion and the H_2O molecules are separately optimized with the DZP CISD or DZP+diff CISD methods. The zero-point corrected energy differences (D_0) are based on the zero-point vibrational energies evaluated using the DZP SCF and DZP+diff SCF methods, and are reported in Table VIII.

For the energetic comparisons with experimental data, the enthalpies changes are evaluated as follows:[22]

$$\Delta H^\circ = D_e + \Delta E_v^\circ + \Delta(\Delta E_v)^{298} + \Delta E_r^{298} + \Delta E_t^{298} + \Delta PV$$

where ΔE_v° is the difference between the zero-point vibrational energies of reactants and product at 0 K; $\Delta(\Delta E_v)^{298}$ is the change in the vibrational energy difference in going from 0 to 298 K. The final terms are for changes in the number of rotational and translation degrees of freedom and the work term.

Entropy changes (ΔS°) have been evaluated from standard statistical mechanical relationships,[23] and finally free energy changes (ΔG°) are calculated. The theoretical values of ΔH°, ΔS°, and ΔG° are reported in Table IX. In all calculations the vibrational frequencies evaluated at the DZP SCF and DZP+diff SCF levels are used. The standard state is 1 atm at 298 K.

Usually, theoretical and spectroscopic absolute entropies agree very well.[23] For example, our theoretical entropy value of water molecule at the DZP+diff SCF level is 45.1 cal/K·mol, exactly the same as experimental value.[23] For the reaction

$$PO_3^- + H_2O \rightarrow PO_3^-\cdot H_2O$$

the agreement between the theoretical ΔS° and the experimental ΔS° is satisfactory. The experimental $-\Delta S^\circ$ reported in ref 2 is 93 ± 4 J/K·mol, with a 10-J/K·mol uncertainty. Thus the experimental upper bound of $-\Delta S^\circ$ is about 25.6 cal/K·mol, while our theoretical $-\Delta S^\circ$ is 25.8 cal/K·mol at the DZP+diff SCF level of theory.

Compared with the experimental enthalpy change[2] ΔH° for the formation of the $PO_3^-\cdot H_2O$ cluster, the theoretical value of $-\Delta H^\circ$ with the DZP SCF method (12.6 kcal mol^{-1}) is slightly lower, while the DZP CISD (14.8 kcal mol^{-1}) and DZP CCSD (15.1 kcal mol^{-1}) methods give values higher than the experimental $-\Delta H^\circ$ (12.9 kcal mol^{-1}).

Closer agreement with the experimental enthalpy change for

$$PO_3^- + H_2O \rightarrow PO_3^-\cdot H_2O$$

(22) Del Bene, J. E.; Mettee, H. D.; Frisch, M. J.; Luke, B. T.; Pople, J. A. *J. Phys. Chem.* **1983**, *87*, 3279.

(23) Hout, R. F. Jr.; Levi, B. A.; Hehre, W. J. *J. Comput. Chem.* **1982**, *3*, 234.

Table IV. Equilibrium Geometries for the Global Minimum Structure of $PO_3^-\cdot(H_2O)_2$ (Figure 7)[a]

theoretical level	r_e (P_1–O_2)	r_e (P_1–O_3)	r_e (O_5–H_7)	r_e (O_5–H_9)	r_e (O_3–H_7)	r_e (O_5–H_6)	θ_e O_3–P_1–O_4	θ_e H_7–O_5–H_9	θ_e P_1–O_3–H_7
DZ SCF	1.564	1.557	0.956	0.957	2.271	2.166	122.9	108.5	105.1
DZ CISD	1.588	1.579	0.972	0.973	2.229	2.140	122.9	107.1	104.8
DZP SCF	1.468	1.461	0.951	0.951	2.224	2.236	121.6	101.7	107.0
DZP CISD	1.483	1.474	0.960	0.961	2.151	2.132	121.8	100.3	105.9
DZP+diff SCF	1.469	1.462	0.951	0.951	2.240	2.252	121.6	102.0	107.1

[a] All bond distances are in Å and angles in deg.

Table V. Harmonic Vibrational Frequencies (cm^{-1}) for the Global Minimum Structure of $PO_3^-\cdot(H_2O)_2$ at the SCF Level of Theory (Figure 7)

mode	symmetry	DZP	DZP+diff	mode	symmetry	DZP	DZP+diff
sym O–H	A_1	4160 (3046)[a]	4155 (3043)[a]	sym def	A_1	546 (546)	541 (541)
asym O–H	B_1	4157 (3044)	4152 (3041)	O–P out-of-plane	B_2	533 (570)	528 (559)
sym O–H	A_1	4095 (2956)	4091 (2952)	asym torsion	B_2	395 (283)	391 (281)
asym O–H	B_1	4093 (2954)	4089 (2951)	asym torsion	A_2	386 (274)	382 (272)
trigonal def	A_1	1846 (1348)	1825 (1332)	asym def	A_1	366 (265)	352 (256)
trigonal def	B_1	1834 (1336)	1814 (1323)	asym def	B_1	365 (260)	352 (251)
asym P–O	B_1	1440 (1445)	1427 (1431)	O···H stretch	B_1	161 (155)	155 (149)
sym P–O	A_1	1405 (1407)	1399 (1397)	O···H stretch	A_1	150 (143)	145 (138)
sym P–O	A_1	1137 (1136)	1132 (1132)	O···H stretch	B_1	95 (93)	90 (88)
puckering	B_2	639 (474)	674 (467)	asym torsion	A_2	51 (51)	47 (47)
puckering	A_2	667 (488)	651 (476)	O···H stretch	A_1	49 (48)	46 (45)
asym def	B_1	555 (555)	551 (551)	asym torsion	B_2	38 (38)	34 (34)

[a] The values in parentheses refer to $PO_3^-\cdot(D_2O)_2$.

is found when diffuse functions are added to the basis set. Specifically, the diffuse functions decrease the CISD $-\Delta H°$ from 14.8 (DZP) to 13.8 kcal mol^{-1} (DZP+diffuse). With the DZP+diffuse CCSD method, $-\Delta H°$ ($PO_3^-\cdot H_2O$) is also predicted to be 13.8 kcal mol^{-1}, indicating that theoretical value may be almost converged.

It is interesting that theory and experiment agree very well for the $\Delta G°$ value for the reaction above. The theoretical $\Delta G°$ at the DZP CCSD, DZP+duff CISD, and DZP+diff CCSD levels are within the stated error bars of Keesee and Castleman's experiment.[2]

Generally, the main error in the theoretical ΔH and ΔS values arises from the harmonic approximation. However, this shortcoming may be partly cancelled in evaluating theoretical ΔG values from the relationship

$$\Delta G = \Delta H - T\Delta S$$

In the case of the reaction above, the change of zero-point vibrational energies $\Delta E_v°$ is 2.3 kcal mol^{-1}, and $\Delta(\Delta E_v)^{298}$ is 1.9 kcal mol^{-1}. The vibrational term contribution to $\Delta S°$ is 14.0 cal/K·mol. Thus the total vibrational contribution to $\Delta G°$ is 0.0 kcal mol^{-1} at 298 K.

This agreement means that the correlated levels of theory describe the reaction very well with respect to $\Delta G°$, providing that vibrational term contributions cancel each other at a particular temperature. However, it is fortuitous that this temperature happened to be 298 K for the reaction above.

There is one apparent discrepancy between theory and experiment in Table IX. Namely, the experimental $PO_3^-\cdot H_2O$ enthalpy change (12.9 kcal mol^{-1}) is greater than the analogous $PO_3^-\cdot D_2O$ value (12.6 kcal mol^{-1}). Theory shows the opposite trend, with the $PO_3^-\cdot H_2O$ enthalpy change being smaller by 0.4 kcal mol^{-1} using the DZP SCF zero-point vibrational energies (ZPVE's) and smaller by 0.2 kcal mol^{-1} with the DZP+diffuse SCF ZPVE's. With the latter basis set the individual ZPVE's are 24.8 kcal mol^{-1} ($PO_3^-\cdot H_2O$), 8.0 kcal mol^{-1} (PO_3^-), 14.5 kcal mol^{-1} (H_2O), 20.3 kcal mol^{-1} ($PO_3^-\cdot D_2O$), and 10.6 kcal mol^{-1} (D_2O). The theoretical results would appear to be more reasonable than the experiments in this regard. The D_2O complex sits lower in the potential minima, and therefore ZPVE effects should be smaller for $PO_3^-\cdot D_2O$ than for $PO_3^-\cdot H_2O$. That is, the theoretical D_0 values for $PO_3^-\cdot D_2O$ are closer to the D_e values than are the $PO_3^-\cdot H_2O$ results.

The overall effect of ZPVE is to make $D_0 < D_e$ since the $PO_3^-\cdot H_2O$ and $PO_3^-\cdot D_2O$ complexes have six more vibrational

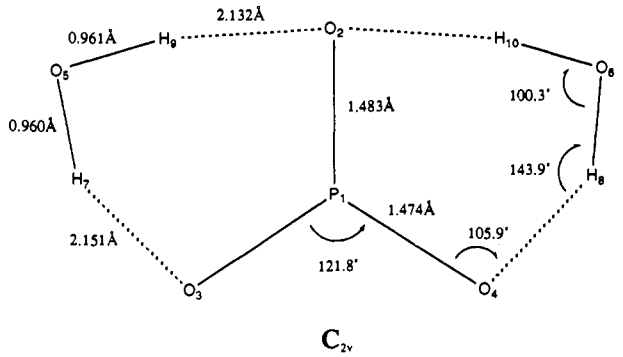

C_{2v}

Figure 7. The global minimum of $PO_3^-\cdot(H_2O)_2$ at the DZP CISD level of theory.

degrees of freedom than do separated $PO_3^- + H_2O$ or $PO_3^- + D_2O$. However, the difference between D_0 and D_e should be less for the D_2O complex than for the H_2O complex. Thus the experimental ordering[2] of $PO_3^-\cdot H_2O$ and $PO_3^-\cdot D_2O$ dissociation energies appears to be incorrect.

C. Metaphosphate Anion–Two Water Clusters, $PO_3^-\cdot(H_2O)_2$. It is important to understand the structure and properties of this cluster. The experiments of Keesee and Castleman[2] have suggested that for the $PO_3^-\cdot(H_2O)_n$ family, $PO_3^-\cdot(H_2O)_2$ is the most reactive cluster in the gas phase. Our results show that PO_3^- and H_2O still have a strong tendency to form double donor–double acceptor hydrogen bonds in this cluster. The theoretical optimized geometries for the global minimum of $PO_3^-\cdot(H_2O)_2$ are given in Figure 7 and Table IV, and the harmonic vibrational frequencies and normal mode assignments in Table V. This global minimum may be thought of as a descendant of Figure 2, the global minimum for $PO_3^-\cdot H_2O$. The hydrogen-bonding structure, the binding energy, and the vibrational frequencies follow the same pattern as predicted for $PO_3^-\cdot H_2O$. In $PO_3^-\cdot(H_2O)_2$, the binding energy for the second water molecule is smaller than that of the first. The frequencies of the new vibrational modes due to the formation of additional hydrogen bonds are generally smaller than those of $PO_3^-\cdot H_2O$ (Table V). The frequency of the A_2''(umbrella) vibrational mode in PO_3^-, which is the O–P out-of-plane mode in $PO_3^-\cdot H_2O$ and $PO_3^-\cdot(H_2O)_2$, decreases as successive water molecules are added.

For the cluster formation step (1, 2), the experiments of Keesee and Castleman[2] were only possible with D_2O. This was not

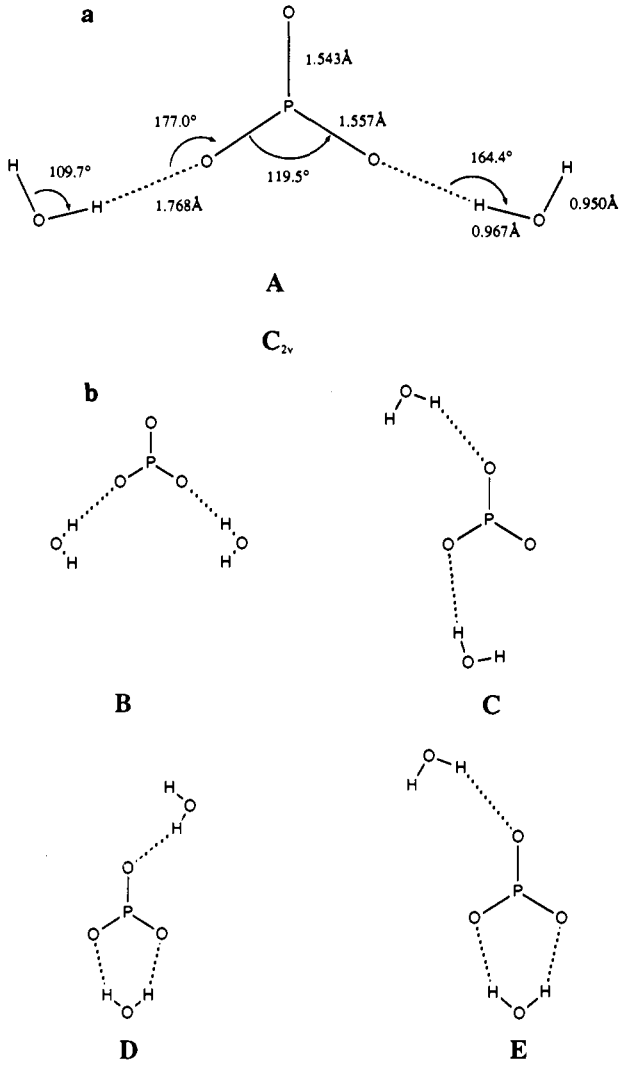

Figure 8. (a) A conformer of $PO_3^-\cdot(H_2O)_2$ with two conventional hydrogen bonds. This structure was obtained at the DZ SCF level of theory. It collapses to Figure 7 at DZP SCF level of theory. (b) Several additional conformations of $PO_3^-\cdot(H_2O)_2$.

expected to be a problem since the experimental dissociation energies of $PO_3^-\cdot H_2O$ and $PO_3^-\cdot D_2O$ differ by only 0.3 kcal mol^{-1}, as discussed above. For the reaction

$$PO_3^-\cdot D_2O + D_2O \rightarrow PO_3^-\cdot(D_2O)_2$$

the experimental $\Delta H°$ value is −11.4 kcal mol^{-1}. Our comparable DZP+diff SCF $\Delta H°$ (−10.8 kcal mol^{-1}) for $PO_3^-\cdot(D_2O)_2$ formation agrees with this deuterated $\Delta H°$ value to within 0.6 kcal mol^{-1}. As was true of the $PO_3^-\cdot D_2O$ complex, the SCF $-\Delta H°$ values are lower than the experimental $-\Delta H°$ for the $PO_3^-\cdot(D_2O)_2$ complex. However, as was also seen for $PO_3^-\cdot D_2O$, the DZP CISD method increases $-\Delta H°$ (1, 2) significantly, to 13.0 kcal mol^{-1}. When the latter prediction is lowered slightly to reflect the effect of diffuse basis functions, the agreement with experiment is quantitative.

Figure 8 gives some structures that appear only at the STO-3G or DZ SCF levels. With the DZP SCF method these structures collapse to Figure 7, the global minimum, and Figure 9, another $PO_3^-\cdot(H_2O)_2$ minimum. This general sort of behavior was also observed in the case of $PO_3^-\cdot H_2O$ discussed above. But unlike $PO_3^-\cdot H_2O$, which has only one structure that is a true minimum, for $PO_3^-\cdot(H_2O)_2$ we find two distinct minima. Note that Figure 9 is a minimum very close to a planar transition state. Because the transition state has a structure almost identical with the minimum, no separate structure is shown for the planar transition state. The particular structure shown in Figure 9 is a minimum because the first H_2O molecule forms double donor–double acceptor hydrogen bonds, thus blocking the site for the second H_2O

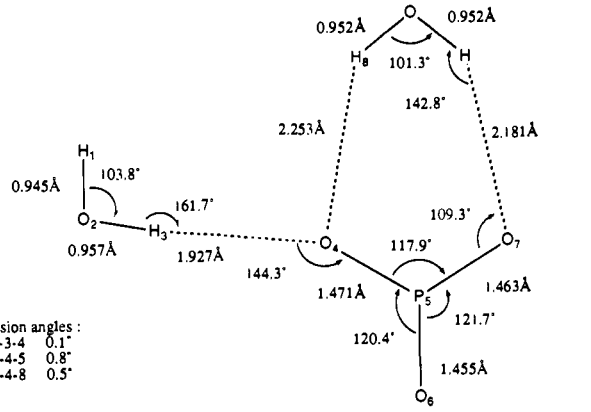

Figure 9. A C_1 minimum of $PO_3^-\cdot(H_2O)_2$ at the DZP SCF level of theory. The structure of the C_s transition state is almost identical except that all atoms are in the same plane.

molecule to form such bonds. The corresponding planar transition state has one imaginary vibrational frequency (15i cm^{-1}), which corresponds to the torsional movements (torsion 1–2–3–4 and torsion 2–3–4–5) of the H_2O molecule distorting from the constrained coplanar symmetry. This imaginary vibrational frequency is so small that removal of the C_s symmetry decreases this torsional angle to a mere 0.8° and the energy difference to 0.000 006 kcal mol^{-1}! Thus there is essentially no structural difference between this local minimum and the planar transition state. This secondary minimum lies 2.1 kcal mol^{-1} higher above the global minimum. Even though the second H_2O forms only one hydrogen bond, there may be a very slight interaction with the oxygen atom O_6. The bond angle O_4–P_5–O_6 is slightly smaller than O_6–P_5–O_7. The P–O bonds behave in the same manner as for $PO_3^-\cdot H_2O$; the two complexed P–O bonds become longer, while the unencumbered bond (P_5–O_6) becomes shorter. This configuration has some character of the valence structure i, but the global minimum (Figure 7) has more of the hypervalent character of ii.

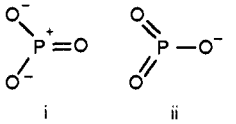

For $PO_3^-\cdot(H_2O)_2$, there is a "true" transition state (Figure 10) similar to the transition state for $PO_3^-\cdot H_2O$ (Figure 4). This structure has one imaginary vibrational frequency, corresponding to the movement of the water molecule toward the global minimum. In the $PO_3^-\cdot(H_2O)_2$ transition state, the three P–O bond lengths are almost equal, suggesting that all three oxygen atoms in the PO_3^- anion experience comparable interactions with the H_2O molecule.

Figure 11 depicts some additional stationary points for $PO_3^-\cdot(H_2O)_2$. It is interesting to note that there can be hydrogen bonding between H_2O molecules within the cluster. One of those structures, C in Figure 11b, has a lower energy than structures D and E in the same figure due to the weak secondary hydrogen bond formed between the two water molecules. Among these $H_2O\cdots H_2O$ stationary points, the most interesting are structures A and B of Figure 11a. The starting points for optimization of the structures reported in Figure 11a were derived from Figure 2, the global minimum for $PO_3^-\cdot H_2O$, plus a second H_2O in the plane perpendicular to the $PO_3^-\cdot H_2O$ plane. When the arrangement of the second H_2O is such that the two hydrogen atoms point toward $PO_3^-\cdot H_2O$, the potential surface leads this water molecule in the direction of structure A in Figure 11a. When the orientation of the second H_2O molecule is such that the oxygen atom in H_2O points toward $PO_3^-\cdot H_2O$ (i.e., the arrangement opposite to that described above), then the potential surface leads this H_2O in the direction of structure B in Figure 11a. In the latter case the second water molecule hydrogen bonds with the water molecule in $PO_3^-\cdot H_2O$ rather than with the PO_3^- moiety. As might be expected, this hydrogen bonding is weaker than that

Table VI. Harmonic Vibrational Frequencies (cm^{-1}) for the D_{3h} Symmetry Global Minimum Structure of $PO_3^-\cdot(H_2O)_3$ at the SCF Level of Theory (Figure 12)

mode	symmetry	DZP	DZP+diff	mode	symmetry	DZP	DZP+diff
sym H–O	E′	4174 (3057)[a]	4169 (3053)[a]	O–P out-of-plane	A_2''	520 (570)	515 (559)
asym H–O	A_2'	4170 (3054)	4166 (3051)	asym torsion	E″	378 (272)	374 (269)
sym H–O	A_1'	4104 (2962)	4100 (2958)	asym def	A_1''	366 (259)	361 (255)
asym H–O	E′	4102 (2960)	4098 (2957)	asym def	E′	354 (253)	339 (242)
trigonal def	A_1'	1845 (1349)	1824 (1334)	asym def	A_2'	354 (259)	339 (249)
trigonal def	E′	1827 (1332)	1808 (1319)	O···H stretch	E′	154 (148)	148 (142)
P–O	E′	1422 (1427)	1412 (1417)	O···H stretch	A_1'	135 (129)	131 (124)
sym P–O	A_1'	1138 (1137)	1134 (1133)	O···H stretch	A_2'	103 (99)	97 (93)
puckering	A_2''	674 (450)	656 (443)	asym torsion	E″	50 (49)	45 (44)
puckering	E″	633 (464)	618 (453)	O···H stretch	E′	45 (44)	42 (41)
asym def	E′	553 (553)	549 (549)	asym torsion	A_2''	27 (26)	23 (23)

[a] The values in parentheses refer to $PO_3^-\cdot(D_2O)_3$.

Table VII. Total Energies and Dissociation Energies for the Global Minimum Structures for $PO_3^-\cdot(H_2O)_n$ Clusters

	total energies (hartrees)			D_e (kcal mol^{-1})			D_0 (kcal mol^{-1})		
theoretical level	$n = 1$	$n = 2$	$n = 3$	$n = 1$	$n = 2$	$n = 3$	$n = 1$	$n = 2$	$n = 3$
DZP SCF	−641.553 29	−717.620 51	−793.685 60	14.5	27.5	39.1	12.1	22.9	32.4
DZP CISD	−642.260 42	−718.471 99	−794.672 41[a]	16.7	31.2	43.5[a]	14.3	26.6	36.8[a]
DZP CCSD	−642.402 06			17.0			14.6		
DZP+diff SCF	−641.565 76	−717.635 17	−793.702 60	13.7	26.1	37.3	11.4	21.6	30.8
DZP+diff CISD	−642.284 20			15.6			13.3		
DZP+diff CCSD[b]	−642.430 91			15.6[b]			13.3[b]		

[a] Single-point evaluations at the DZP SCF optimized geometries. [b] Single-point evaluations at the DZP+diff CISD optimized geometries.

of the former case, but it is still significant.

The DZP SCF total energy of the structure B in Figure 11a is −717.616 24 hartrees. Since the total energy of H_2O is −76.046 55 hartrees and the total energy of the structure for the global minimum of $PO_3^-\cdot H_2O$ in Figure 2 is −641.553 29 hartrees at the same theoretical level, the binding energy for the second H_2O attaching to the first H_2O is 10.3 kcal mol^{-1}. Thus the $PO_3^-\cdot H_2O$–H_2O binding energy is almost twice as large as that of the water dimer. It is interesting to note the geometry change within $PO_3^-\cdot H_2O$ after it binds with the second water molecule to form $PO_3^-\cdot H_2O$–H_2O. For $PO_3^-\cdot H_2O$, the hydrogen bond length is 2.197 Å and the O_3–P_1–O_4 bond angle is 118.4° at the DZP SCF level (Table II), but the corresponding values for $PO_3^-\cdot H_2O$–H_2O are 2.116 Å and 117.8°. This suggests that the formation of the second hydration product increases the interaction between the anion and the first water molecule.

Figure 11c shows the energies of these five stationary points relative to the global minimum for $PO_3^-\cdot(H_2O)_2$. Structure A in Figure 11a has a lower energy than the structure in Figure 9, a minimum of $PO_3^-\cdot(H_2O)_2$. Clearly this is a result of the different orientations of the second water molecule. In Figure 9, the oxygen atom O_6 is free, whereas for the structure A in Figure 11a, all three oxygen atoms in the PO_3^- anion directly participate in hydrogen bonding.

D. Metaphosphate Anion–Three Water Clusters, $PO_3^-\cdot(H_2O)_3$. It is found that for the family of reactions

$$PO_3^-\cdot(H_2O)_n + H_2O \rightarrow PO_3^-\cdot(H_2O)_{n+1}$$

mass spectrometry[2] confirms the presence of the six hydrogen atoms expected for $PO_3^-\cdot(H_2O)_3$. For the cluster formation step $(n, n + 1)$

$$PO_3^-\cdot(H_2O)_n + H_2O \rightarrow PO_3^-\cdot(H_2O)_{n+1}$$

some experimental peculiarities[2] are exhibited in step (2, 3). The enthalpy change $-\Delta H$ is significantly higher in this step than in steps (0, 1) and (1, 2), and the reaction rate is slower. The experimentalists (who used D_2O instead of H_2O for their observations) explain the abnormality in ΔH as being due to the isomerization

$$PO_3^-\cdot(H_2O)_2 + H_2O \rightarrow H_2PO_4^-\cdot(H_2O)_2 \qquad (1)$$

The present theoretical investigation confirms that $PO_3^-\cdot(H_2O)_3$ is a stable species, as indicated in Figure 12. The theoretical structure of D_{3h} symmetry appears consistent in structure, vi-

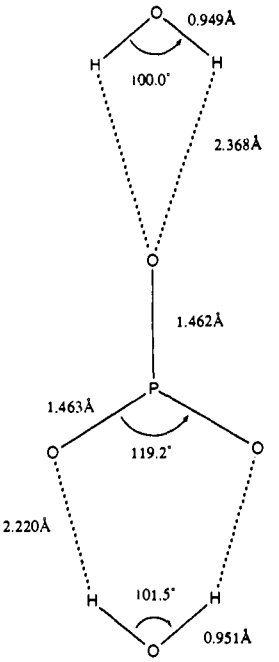

C_{2v}

Figure 10. A transition state for $PO_3^-\cdot(H_2O)_2$ optimized at the DZP SCF level of theory.

Table VIII. Zero-Point Vibrational Energy Corrected Energy Changes for the Formation of the $PO_3^-\cdot(H_2O)_n$ Clusters (kcal mol^{-1})[a]

	theoretical ΔE_0				
$(n, n + 1)$[b]	DZP SCF	DZP CISD	DZP CCSD	DZP+diff SCF	DZP+diff CISD
(0, 1), H_2O	12.1	14.3	14.6	11.4	13.3, (13.3)[c]
(0, 1), D_2O	12.7	14.9	15.2	11.9	13.8, (13.8)[c]
(1, 2), H_2O	10.7	12.1		10.2	
(1, 2), D_2O	11.3	12.6		10.7	
(2, 3), H_2O	9.6	10.2		9.2	
(2, 3), D_2O	10.1	10.8		9.7	

[a] Based on the geometries for the global minima of the clusters. [b] Refers to the reactions: $PO_3^-\cdot(H_2O)_n + H_2O = PO_3^-\cdot(H_2O)_{n+1}$. [c] DZP+diff CCSD level of theory, assuming DZP+diff CISD stationary point geometries.

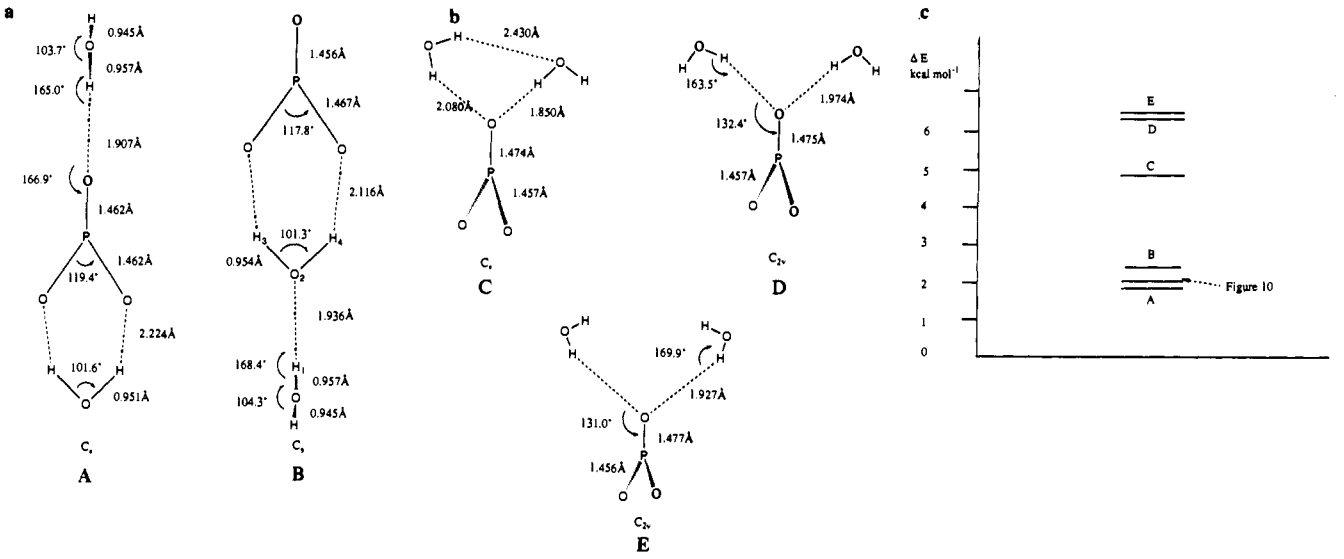

Figure 11. (a) Two stationary points of $PO_3^-\cdot(H_2O)_2$ obtained at the DZP SCF level of theory. In both cases the C_s symmetry plane contains the P–O bond and the out-of-plane H_2O molecule. (b) Additional stationary points for $PO_3^-\cdot(H_2O)_2$ optimized at the DZP SCF level of theory. The symmetry planes contain two H_2O molecules and the P–O bond. (c) The energies of the stationary points shown in (a) and (b) relative to the global minimum of $PO_3^-\cdot(H_2O)_2$ (Figure 7).

Table IX. Thermochemical Data for the Formation of the $PO_3^-\cdot(H_2O)_n$ Clusters[a]

	DZP SCF			DZP+diff SCF			DZP CISD		DZP CCSD		DZP+diff CISD[c]		experimental data[d]		
$(n, n+1)$[b]	$-\Delta H°$	$-\Delta S°$	$-\Delta G°$	$-\Delta H°$	$-\Delta S°$	$-\Delta G°$	$-\Delta H°$	$-\Delta G°$	$-\Delta H°$	$-\Delta G°$	$-\Delta H°$	$-\Delta G°$	$-\Delta H°$	$-\Delta S°$	$-\Delta G°$
(0, 1), H_2O	12.6	26.2	4.8	11.9	25.8	4.2	14.8	7.0	15.1	6.2	13.8	6.1	12.9	22.3	6.3
(0, 1), D_2O	13.0	26.7	5.0	12.1	26.3	4.3	15.2	7.2	15.5	6.4	14.0	6.2	12.6	20.8	6.4
(1, 2), H_2O	11.1	27.5	2.9	10.6	27.0	2.5	12.7	4.5							
(1, 2), D_2O	11.5	27.9	3.1	10.8	27.6	2.6	13.0	4.6					11.4	22.0	4.9
(2, 3), H_2O	9.9	28.8	1.3	9.5	28.1	1.1	10.5	1.9							
(2, 3), D_2O	10.2	29.1	1.5	9.7	28.6	1.2	11.1	2.4					16.3	36.4	5.5

[a] Based on the geometries for the global minima of the clusters. The values of ΔH and ΔG are in kcal mol^{-1}, and ΔS in cal/K·mol. The standard state is 1 atm at 298 K. [b] Refers to the reactions: $PO_3^-\cdot(H_2O)_n + H_2O = PO_3^-\cdot(H_2O)_{n+1}$. [c] The values are the same as the DZP+diff CCSD level of theory, assuming DZP+diff CISD stationary-point geometries. [d] Keesee and Castleman, ref 2.

brational frequencies (Table VI), and characteristics of hydrogen bonding with the smaller complexes $n = 1$ or 2.

We must be careful to state that Keesee and Castleman[2] in no way exclude the possibility of a D_{3h} minimum for $PO_3^-\cdot(H_2O)_3$. They do say (as confirmed here by theory) that the third dissociation energy (2, 3) for D_{3h} $PO_3^-\cdot(H_2O)_3$ should be less than that for (0, 1) and (1, 2). On this basis Keesee and Castleman conclude that their data are best explained by an isomerization from the D_{3h} $PO_3^-\cdot(H_2O)_3$ minimum to a lower energy structure, plausibly $(HO)_2PO_2^-\cdot(H_2O)_2$.

The D_{3h} equilibrium geometry of Figure 12 confirms that all of the $PO_3^-\cdot(H_2O)_n$, $n = 1$, 2, and 3, structures are of the double donor–double acceptor type. This is not an intuitively required result. For example, in their thoughtful and excellent analysis, Keesee and Castleman[2] assume linear hydrogen bonds of length 1.5 Å. New experiments to confirm or deny these fresh theoretical structures would certainly be welcome.

Figure 13 shows two configurations that exist only on the STO-3G and DZ SCF potential energy hypersurfaces. Both of these stationary points collapse to the global minimum D_{3h} structure at the DZP SCF level. We find that polarization basis functions are important in determining the nature of the hydrogen bonding in the clusters. For example, even when electron correlation effects are considered at the DZ CISD level, the C_{2v} symmetry $PO_3^-\cdot(H_2O)_3$ in Figure 13, A, does not collapse to the D_{3h} structure.

In a manner similar to $PO_3^-\cdot(H_2O)_2$, the lowest vibrational frequencies due to hydrogen bonding continue to decrease for $PO_3^-\cdot(H_2O)_3$. The smallest DZP SCF harmonic vibrational frequency is 27 cm^{-1}, and the addition of diffuse basis functions reduces this result to 23 cm^{-1}.

In one of the earliest ab initio studies of PO_3^-, Loew suggested that PO_3^- may be both an electrophile and an anion,[24] because

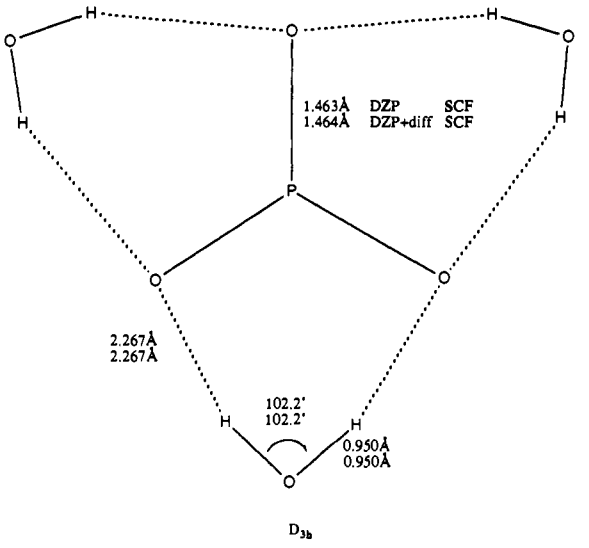

Figure 12. The global minimum equilibrium geometry for $PO_3^-\cdot(H_2O)_3$.

there is a positive charge "hole" in phosphorus. Of course, the preferred approach for a nucleophile is along a path perpendicular to the molecular plane. But Henchman refuted this possibility based on his experiments.[1] In our research, for $n = 1$, 2, and 3, we have tried to locate some stationary points for which the oxygen atom in a water molecule can approach the phosphorus atom along the axial path perpendicular to the PO_3^- plane. However, our results do not support such a possibility. In the C_{2v} coplanar

(24) Loew, L. M.; MacArthur, W. R. J. Am. Chem. Soc. 1977, 99, 1019.

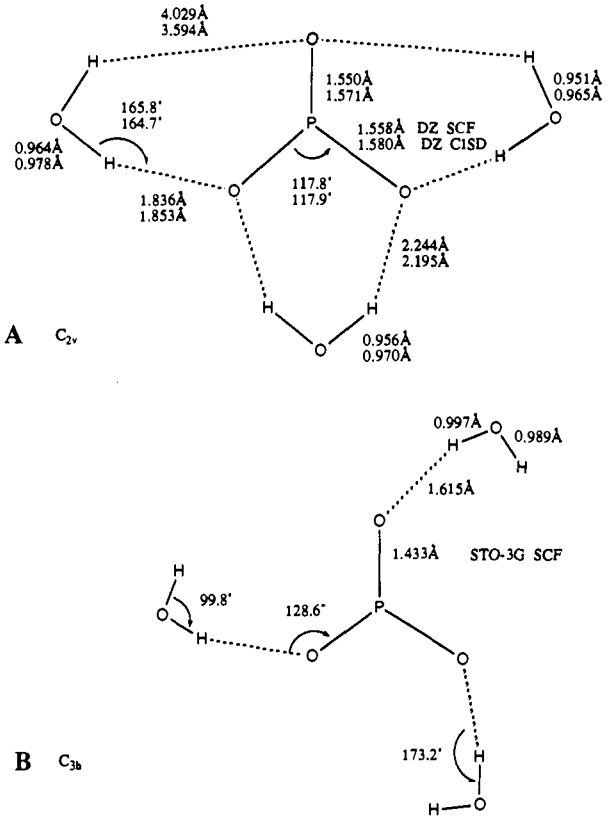

Figure 13. Two structures of $PO_3^-\cdot(H_2O)_3$ predicted at the STO-3G SCF and DZ SCF levels of theory. Both structures collapse to the higher symmetry structure of Figure 12 at the DZP SCF level of theory.

approach, as the lone pair of the water oxygen atom moves toward PO_3^-, the H_2O remains far away; i.e., there is no stationary point for such orientation at the DZP SCF level. This situation is no better in the axial direction, and even for $n = 2$, where the third water molecule may have a greater chance to approach in this manner, the result is still negative. As previously mentioned (Figure 11a) in forming $PO_3^-\cdot(H_2O)_3$, we may suppose that the $PO_3^-\cdot(H_2O)_2$ collides with the third H_2O molecule in different orientations. The different orientations lead to the "products" in Figures 14 and 15, respectively. In both Figure 14 and 15, it may be seen that the oxygen atom in PO_3^- cannot afford to form hydrogen bonds with three hydrogen atoms as a triple acceptor. The approach of the third H_2O "breaks" some of the previously formed hydrogen bonds, and monodonor hydrogen bonding is preferred for these two stationary points. There is little difference between these two structures (Figures 14 and 15). Except for the orientation of the H_2O moieties, the PO_3^- anion is unchanged under the influence of these two different H_2O approaches. These two stationary points lie about 4.6 and 4.4 kcal mol^{-1} higher than the global minimum, respectively.

4. Conclusions

In this paper we have presented detailed theoretical studies of the $PO_3^-\cdot(H_2O)_n$ clusters. The highest theoretical level used is the DZP+diff CCSD method. For $n = 0$, 1, 2, and 3, the global minima are shown in Figures 1, 2, 7, and 12, respectively. The theoretical results confirm the presence of $PO_3^-\cdot(H_2O)_n$ clusters found experimentally. Our most important result is that the clusters tend to form high-symmetry double donor hydrogen bonds between the PO_3^- anion and the H_2O molecules. The hydrogen-bond lengths are 2.1–2.2 Å. The hydrogen bond in $PO_3^-\cdot H_2O$ is very comparable to that for $NO_3^-\cdot H_2O$. It is also interesting that the hydrogen bonds can be formed *between* the H_2O moieties in the cluster; these have larger binding energies than that for the isolated water dimer. The theoretical results agree quantitatively with the experimental thermochemistry[2] for the reaction steps (0, 1) and (1, 2). However the third water molecule in the D_{3h} $PO_3^-\cdot(H_2O)_3$ equilibrium structure is significantly less strongly bound than observed. This prediction is consistent with the intuitive analysis of Keesee and Castleman.[2] Whether there is a lower energy $PO_6H_6^-$ isomer such as $(HO)_2PO_2^-\cdot(H_2O)_2$ remains an important unresolved question.

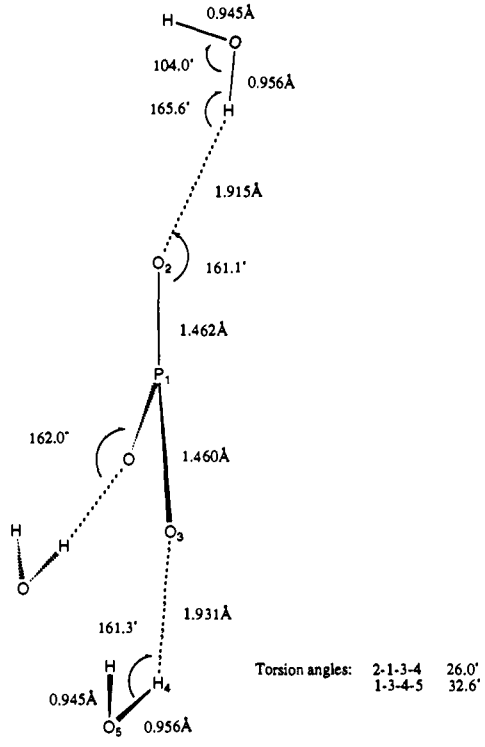

Figure 14. Another stationary point for $PO_3^-\cdot(H_2O)_3$ optimized at the DZP SCF level of theory. The C_s symmetry plane contains the upper H_2O molecule and the in-plane P–O bond.

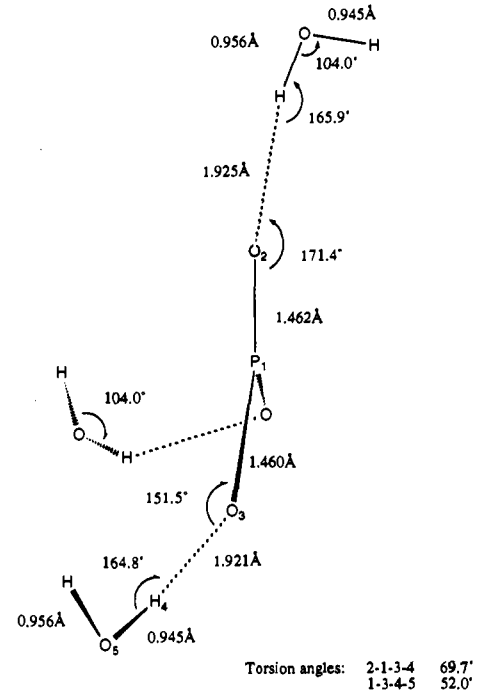

Figure 15. A final stationary point for $PO_3^-\cdot(H_2O)_3$ obtained at the DZP SCF level of theory. The C_s symmetry plane contains the upper H_2O molecule and the in-plane P–O bond.

Acknowledgment. Helpful discussions with Dr. Y. Yamaguchi, Mr. Ching-han Hu, Mr. C. A. Richards, Jr., and Ms. Cynthia Meredith are greatly appreciated. This research was suggested by Drs. Michael Henchman, John Paulson, and Albert Viggiano. The work was supported by the U. S. Air Force Office of Scientific Research under Grant No. AFOSR-92-J-0047.